Journal of Non-Crystalline Solids 356 (2010) 1310–1314

Contents lists available at ScienceDirect

Journal of Non-Crystalline Solids

journal homepage: www.elsevier.com/ locate/ jnoncrysol

Inherent strength of zirconium-based bulk metallic glass

A.S. Bakai [a], A.P. Shpak [b], N. Wanderka [c], S. Kotrechko [b], T.I. Mazilova [a], I.M. Mikhailovskij [a,*]

[a] National Scientific Center "Kharkov Institute of Physics and Technology", Kharkov, 61108, Ukraine
[b] Kurdyumov Institute for Metal Physics, National Academy of Sciences of the Ukraine, Kyiv, 142, 03680, Ukraine
[c] Helmholtz-Zentrum Berlin für Materialien und Energie, Berlin, D-14109, Germany

ARTICLE INFO

Article history:
Received 18 May 2009
Received in revised form 10 February 2010

Keywords:
Atomic structure;
Bulk amorphous metals;
Strength

ABSTRACT

The polycluster morphology and inherent tensile strength of bulk metallic glass $Zr_{41}Ti_{14}Cu_{12.5}Ni_{10}Be_{22.5}$ in the as-cast state were determined by means of high-field mechanical loading using field ion microscopy. The two-level cluster structure with the length scale of the order of 2 and 10 nm was revealed. It was disclosed that the strength of this alloy is characterized by a strong size-effect in a nanometer scale range. It is shown that within this size region the Weibull distribution is not suitable to describe the scale effect. It is ascertained that the limit level of shear strength of the examined glass is 5.8 GPa, and shear strength of a separate cluster may be estimated as 6.7 GPa.

1. Introduction

The inherent strength is the highest achievable strength of defect-free material at 0 K. Conventional crystalline materials fracture at stresses far below its theoretical strength and the macroscopic strength is highly sensitive to the specimen size. As it was shown in earlier experiments, the tensile strengths of Fe whiskers [1] and W nanotips [2] are more than an order of magnitude higher than that of the bulk crystals. Recently the determination of theoretical strength became possible using quantum-mechanical electronic structure calculations based on the density functional theory. The calculation results are in harmony with these experiments [3–5].

Metallic glasses provide higher strength and hardness compared to crystalline solids. The origin of the very high tensile strength of the amorphous alloys is shown to be due to a uniform distribution of some kind of atomic clusters [6–8]. In the absence of intrinsic defects such as stacking faults and dislocations, the strength of metallic glasses has been considered to be close to the ideal strength of solids [9,10] However, the existence of extrinsic casting defects (voids, oxides, inclusions, inner boundaries, etc.) makes it difficult to determine the elastic limit of metallic glasses.

Our understanding of the elastic–plastic transition and strain-releasing mechanism on the nanoscale has been dramatically advanced by nanoindentation studies of plastic yielding in defect-free regions under the indenter nanotip. The recent nanoindentation experiments showed that the onset of yielding of metallic glasses in the small volume beneath the indenter is observed at the stresses near the theoretical strength [10,11]. Another promising approach in the determination of the ideal strength of metallic glasses is the use of nanosized specimens, which may be defect-free if the native defect density is low enough. An experimental determination of the tensile strength of nanospecimens is rather challenging, due to the difficulties in measuring the mechanical response of nanoscale objects under tensile load. Because of these problems, there are only a few data about mechanical properties of individual nano-objects, and until now the direct tensile strength measurements of metallic glasses are lacking. In this paper we present results of determination of the tensile strength of zirconium-based bulk metallic glass by the high-field method of mechanical loading using field ion microscopy (FIM) [2,12].

2. Experimental details and material

A zirconium-based bulk metallic glass (BMG) $Zr_{41}Ti_{14}Cu_{12.5}Ni_{10}Be_{22.5}$, Vitreloy 1 (V1) was used in the current investigation. Amorphous ingots of 12 mm in diameter were produced by alloying of pure constituents in an inductive levitation furnace under the argon atmosphere by re-melting several times. The amorphous nature and large-scale homogeneity of the as-quenched material were verified by means of X-ray diffraction, small angle neutron scattering and transmission electron microscopy. Thin disks of 0.2 mm were cut from the ingots. In order to perform FIM analysis the samples were cut into the rods of $10\times0.2\times0.2$ mm using a diamond wire saw. Needle-like specimens with an initial radius of the curvature r_0 of about 10 nm at a hemispherical top (Fig. 1(a)) were electrolytically polished in a solution of 10% $HClO_4$ + 90% CH_3COOH at room temperature and at DC voltage of 12–15 V. The specimen surface was cleaned and polished *in situ* by the methods of field desorption and by low-temperature field evaporation in a FIM [12].

FIM experiments were performed at 77 K with a two-chamber field emission microscope operating in the ion and electron regimes. The

* Corresponding author. Tel.: +380 57 700 2676; fax: +380 57 335 1688.
E-mail address: mikhailovskij@kipt.kharkov.ua (I.M. Mikhailovskij).

0022-3093/$ – see front matter © 2010 Elsevier B.V. All rights reserved.
doi:10.1016/j.jnoncrysol.2010.03.009

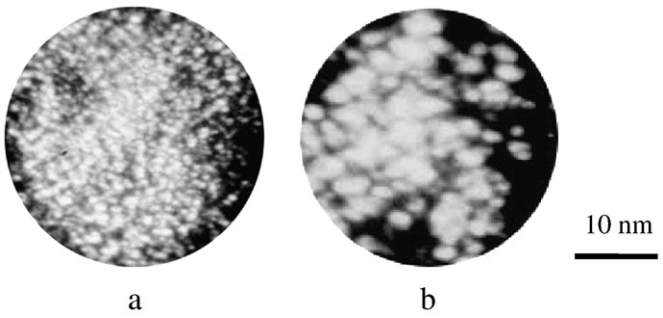

Fig. 1. Field ion microscopic images of the $Zr_{41}Ti_{14}Cu_{12.5}Ni_{10}Be_{22.5}$: (a) after pulsed field evaporation at a rate of about 1 nm s^{-1}. (b) After hydrogen promoted field etching.

microscope was evacuated by a cryogenic pump to residual gas pressure of 10^{-6} Pa. For the imaging the mixture of 90% He and 10% H_2 or Ne at a pressure of 10^{-4}–10^{-2} Pa was used in this study. In the field ion- and electron mode the applied voltage U_{dc} on the specimen was in the range between 3 and 20 kV and the applied U_{ac} voltage varied between 6 and 25 kV, respectively. The amplitude of negative voltage pulses of about 10^{-3} s was sufficient for creating on the sample surface an electric field strength corresponding to a field electron emission density of 10^2–10^3 A cm^{-2}. In order to reduce the intensity of ionic bombardment of the surface a microchannel amplifier was used to record the electron images at low densities of the field electron current. A mechanical loading was applied by a high voltage pulse with a pulse length of 1.5×10^{-7} s at a level of 0.8 of the amplitude. The voltage pulse U_p was varied from 0.5 to 10 kV. In order to eliminate the vacuum discharges initiated by the field electron emission and evaporation of the electrodes a voltage of up to 25 kV was applied to the specimen holder in FIM without the specimen [13].

Some of the experiments were also performed at 60 K with an atom probe field ion microscope (AP/FIM) with a high voltage pulse of 4×10^{-9} s at a vacuum below 10^{-10} Pa. The high voltage pulse applied to the specimen can produce a multiplication of pulse voltage under reflection conditions. The total operation voltage U is equal to $U_{dc}+\beta U_p$, where β is a pulse enhancement factor which depends on the geometry of the specimen holder assembly and has a value between 1 and 2. A high frequency component of the total voltage was attenuated by inductance and capacitance in the pulse line. Both these effects cannot be quantitatively appreciated. Therefore, the pulse enhancement factor was determined *in situ* experimentally. The calibration was based on a control compensation of the reduction of pulse voltage fraction by the increase of the constant DC voltage. The constancy of the resulted voltage was controlled by reaching the onset field of a low-temperature evaporation of specimens.

The tensile strength was determined by the method of loading by electric field in FIM [2,12]. This method is based on the arising of mechanical stress on the surface of a conductor in strong electric fields. An electric field F acting at the surface of a specimen produces a normal stress $\varepsilon_0F^2/2$, where ε_0 is permittivity of free space. Due to high electric fields employed in FIM, the mechanical stress on the specimen surface may approach the theoretical strength. The stress distribution is rather complex and consists of both shear and normal components. However at a distance much larger than the radius of the specimen curvature the load is nearly uniaxial. In the case of FIM investigations of non-crystalline materials the local magnification is unknown and the electric field strength may be determined by comparison with the onset field of low-temperature evaporation or field of the best image. A radius of the specimen r_0 was determined by the known evaporation electric field F of the alloying elements and the value of the voltage U applied to the specimen:

$$F = U/kr_0, \tag{1}$$

where k is the field enhancement factor [12]. It should be pointed out that the deviation of the shape of the specimen from the spherical has no influence on the field enhancement factor, since the distance between a sample and a fluorescent screen is 10^5–10^6 times larger than the radius of the investigated part of the samples.

It is usually assumed that the tip is smooth and axially symmetrical, and that it may be described as a curved surface $r=R(z)$ in cylindrical coordinates where the z is the coordinate along the specimen axis. The field-induced stress acting over the specimen surface from the apex to the plane $z=z_0$ produces the force on the plane in the z direction given by:

$$f_z = \frac{1}{2}\iint \varepsilon_0 F^2 \cos\gamma dS, \tag{2}$$

where dS is an element of surface area, γ is the angle between the z axis and the normal to that element. The integral is taken over the whole specimen surface with $0<z<z_0$. The average stress can be calculated by integration of the field-induced stress on the specimen surface and dividing by the area of the section concerned. Electric field calibration was based on the comparison with the best image field and voltage in the field ion microscope operated with He, Ne, and H_2 [14].

The shape and radii of curvature of the top parts of the samples were analyzed using an optical microscope and a transmission electron microscope (TEM) Philips EM400 with the operating voltage of 100 kV. To image the structure of the BMG we employed a high-resolution transmission electron microscope (HRTEM) JEOL JEM-4000EX (II).

3. Results

Typical FIM images of Zr-based V1 in the as-cast state are shown in Fig. 1. Disorderly located bright spots observed in the FIM images correspond to individual atoms (Fig.1(a)) and small atomic clusters (Fig. 1(b)). No indications of a regular crystal structure are visible. Random distribution of the bright spots indicates that the arrangement of atoms does not have a structural order.

In the case of field evaporation rate about 1 nm s^{-1} under He–H_2 gas mixture the ion image of the amorphous alloy is an isotropic set of emission centers (Fig. 1(a)). However, when the rate of field evaporation is decreased to 10^{-2} nm s^{-1}, the selective field etching reveals the structural heterogeneities of the amorphous alloy. Fig. 1(b) shows compact nanometer-sized atomic complexes-subclusters surrounded by regions with reduced image brightness. The close-packing of atoms in these complexes is evident, in particular the absence of point resolution which is usually typical for FIM images of the most close-packed group of atoms on the surface [15]. The size distribution of the subclusters shown in Fig. 2 has a maximum at 2 nm. The inset in Fig. 2 shows HRTEM image of the $Zr_{41}Ti_{14}Cu_{12.5}Ni_{10}Be_{22.5}$ alloy in the as-cast state. Such images correspond to homogeneous solids free of inclusions and microcracks.

The sizes of regions with medium-range ordering in metallic glasses as reported previously in [6,16,17] are of similar order of magnitude. In contrast to field ion images the field electron images of V1 reveal substantial variations of the field emission formed by low-temperature field evaporation [18]. The peculiarities of field electron contrast observed in Fig. 3 correspond to the local variations of the evaporation energy Q_e, with a characteristic scale of about 10 nm, which indicates the presence of structural heterogeneities. Such heterogeneities are typical for the polycluster structure of metallic glasses [6,18]. The contour diagram of the constant brightness levels (from strong 1 to low 5) for field electron image shown in Fig. 3(b) was plotted using the method described in Ref. [19].

The difference between the local energies of field evaporation for sites of the specimen, which correspond to the neighboring contour lines of constant brightness in Fig. 3(b) is equal to $\Delta Q_e/Q_e=(1.1\pm0.3)\times10^{-2}$. The maximal deviations of a local energy of field evaporation